TECHNICAL MEMORANDUM

228

Note on the sea state dependence of the ocean surface albedo

P. Janssen, B. Becker and J-J. Morcrette

Research Department

May 1996

European Centre for Medium-Range Weather Forecasts
Europäisches Zentrum für mittelfristige Wettervorhersage
Centre européen pour les prévisions météorologiques à moyen

ABSTRACT

In this note we discuss possible consequences of a sea-state dependent ocean surface albedo on simulations of the climate of an atmospheric model. Based on results of *Cox and Munk* (1954) and *Saunders* (1967) we study in two dimensions (hence sunlight and ocean waves propagate in the same plane) the impact of the sea state on the ocean albedo. For high zenith angles a considerable dependence of ocean albedo on sea state is found. Results from a one year simulation of the atmospheric climate by means of cy13r1 of ECMWF's atmospheric model with a sea state dependent albedo show a small impact on the radiation budget and a modest impact on the net heat flux (10 Wm^{-2}), in particular in the Northern Hemisphere. No impact was found on the mean scores of a number of 10 day forecasts.

1. INTRODUCTION

We have studied the dependence on sea state of the albedo of the ocean surface for visible light. We are mainly concerned with the clear sky problem - no pollution, no secondary scattering and the like - so it is assumed that sunlight is a plane wave that hits the ocean surface at zenith angle θ. In the main part of this note only specular reflection of the sunlight from the ocean surface is considered, disregarding the light scattered from whitecaps and the light reflected from substances in the ocean (the "underlight"). Furthermore, we assume geometrical optics, hence we disregard curvature effects so that, on scales of the order of a wavelength of light, the ocean surface may be regarded as flat. The relevant geometry and angles are given in Fig 1.

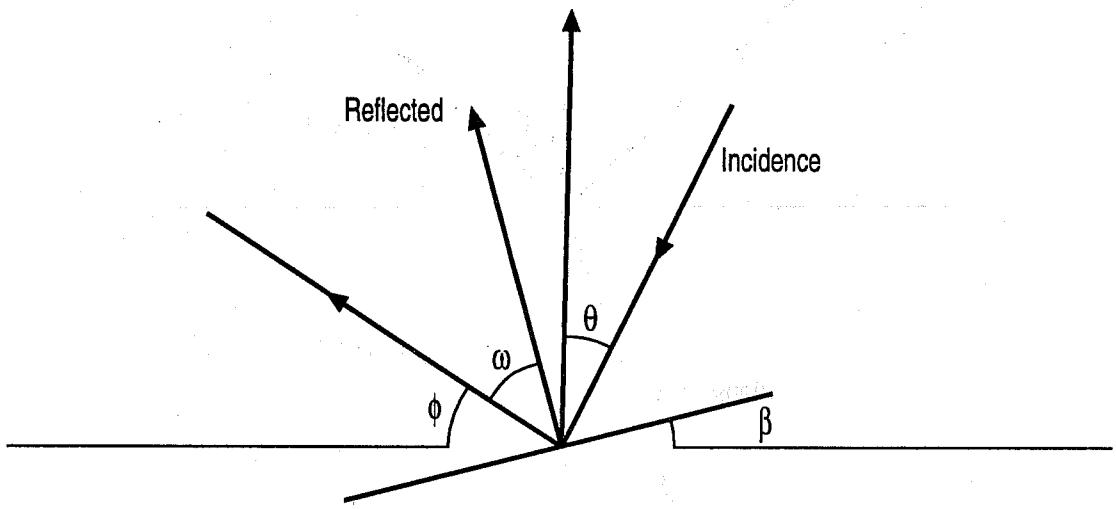

Fig 1 Definition of geometry and angles.

Since albedo is the ratio of reflected and incident sunlight energy, the question of interest is how much of the incident sunlight is reflected back into the atmosphere and does the albedo depend on the sea state?

This question is of interest because in earlier versions of the ECMWF model the albedo was assumed to be independent of the sun's zenith angle. This assumption is an over-simplification because it is known that for a flat surface the albedo should increase with increasing zenith angle, and in the limit the albedo even becomes 1 (since the ocean may be regarded as nonconducting for these wavelengths). Some aspects of reflection at a smooth surface

are discussed in section 2. In practice the ocean surface is not smooth because of the presence of ocean waves. This not only affects the local incidence angle of the sunlight (cf Fig 1) but may also cause shadowing by the ocean waves for high zenith angles. The sea-state dependence of the ocean albedo is discussed in sections 3 and 4. In section 5 we discuss additional relevant effects such as whitecaps and the underlight, while in section 6 the impact of a new albedo formulation on the atmospheric state is discussed. Finally, section 7 summarises our conclusions.

We remark that much of what we discuss uses well-established results: *Cox and Munk* (1954), *Saunders* (1967), *Payne* (1972), *Preisendorfer and Mobley* (1986) and *Mobley* (1994).

2. REFLECTION AT A SMOOTH SURFACE

Here we briefly recall the results of reflection of light at a smooth surface. The media (air and water in our case) are non-conducting and the permeability of the media is that of free space, $\mu=\mu_0=4\pi 10^{-7}$. The reflection and transmission of light at such a surface follows from Maxwell's equations and can be found in many textbooks.

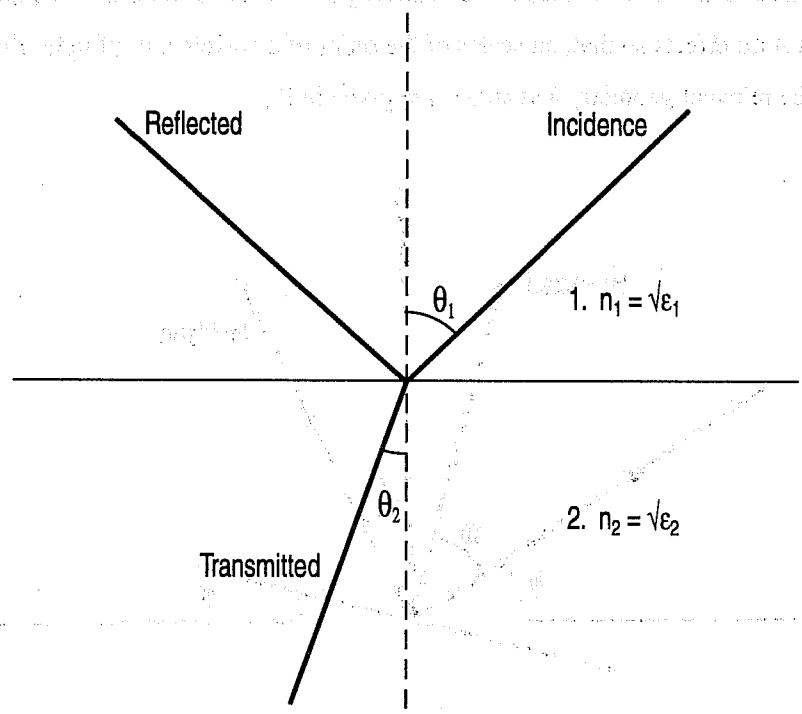

Fig 2 Plane of incidence and definition of angles and refraction index.

Geometry and angles are defined in Fig 2. From Maxwell's equations one finds that the reflected angle equals the incidence angle while the angle of transmitted light follows from Snel's law:

$$\sin\theta_2 = \frac{1}{r}\sin\theta_1,\ r \equiv \frac{n_2}{n_1} \qquad (1)$$

and the ratio of refraction indices for our problem (visible light and water) is r=1.334. Because r is larger than 1 the transmitted light refracts towards the normal, and total reflection (except for $\theta_1 = \pi/2$) does not occur.

The reflective properties of light depend on its polarisation. For example, when the electric field vector is in the plane of incidence the reflection coefficient decreases with incidence angle until it becomes zero at the Brewster angle ($\tan\ \theta_1 = r$) after which it rapidly increases to 1 for $\theta_1 = \pi/2$. On the other hand, when the electric field vector is normal to the plane of incidence the reflection coefficient is minimal at normal incidence and increases monotonically with increasing angle becoming 1 for $\theta_1 = \pi/2$. We assume that the sunlight is not polarised (thus we have a mixture of the two polarisations), however it should be clear that the reflected light is to some extent polarised. As a result, the reflection coefficient of sunlight is the mean of the reflection coefficients of the two polarisation cases,

$$R = \tfrac{1}{2}(R_1 + R_{11}) \tag{2}$$

where

$$R_1 = \left[\frac{\sqrt{r^2-\sin^2\theta_1}-r^2\cos\theta_1}{\sqrt{r^2-\sin^2\theta_1}+r^2\cos\theta_1}\right]^2$$

$$R_{11} = \left[\frac{\sqrt{r^2-\sin^2\theta_1}-\cos\theta_1}{\sqrt{r^2-\sin^2\theta_1}+\cos\theta_1}\right]^2$$

Reflection according to Eq (2) is known as Fresnel reflection. The zenith-angle dependence of R for the smooth case, which corresponds to an rms slope $\sigma=0$, is shown in Fig 3. It is clear that the albedo of a smooth surface depends, to a considerable extent, on the zenith angle, ranging from $[(r-1)/(r+1)]^2 \simeq 0.0204$ for normal incidence to 1 for grazing angles ($\theta_1 \Rightarrow \pi/2$).

It is of interest to compare the albedo for a smooth surface with observations. Morcrette (pers. comm.) has plotted the clear sky planetary albedo over the ocean from ERBE data as a function of the solar zenith angle. His results are given in Fig 4 and we have included the curve for Fresnel reflection. The data show for low solar zenith angles a mean albedo of about 0.1 with hardly any scatter around the mean, while for zenith angles larger than 60° there is considerable scatter. We also remark that the clear sky planetary albedo is always larger than the ocean surface albedo because the sunlight may also be reflected by scattering elements in the atmospheric column. We therefore compare modelled albedos with the lower envelope of the observed planetary albedo because the lower data are closest to a clear sky surface albedo. This seems to be a valid procedure for the lower zenith angles, in particular; however, owing to the large scatter, this may be a questionable approach for the higher zenith angles.

Comparing the Fresnel reflection now with the ERBE data it is concluded that there are considerable discrepancies to be noted. For low zenith angles, Eq (2) gives too low values. This discrepancy may be resolved by the inclusion of 'underlight', while in case of tropical storms whitecaps may be important. It is also clear Fresnel reflection has a more sensitive dependence on zenith angle than the ERBE data. In addition, it is noted

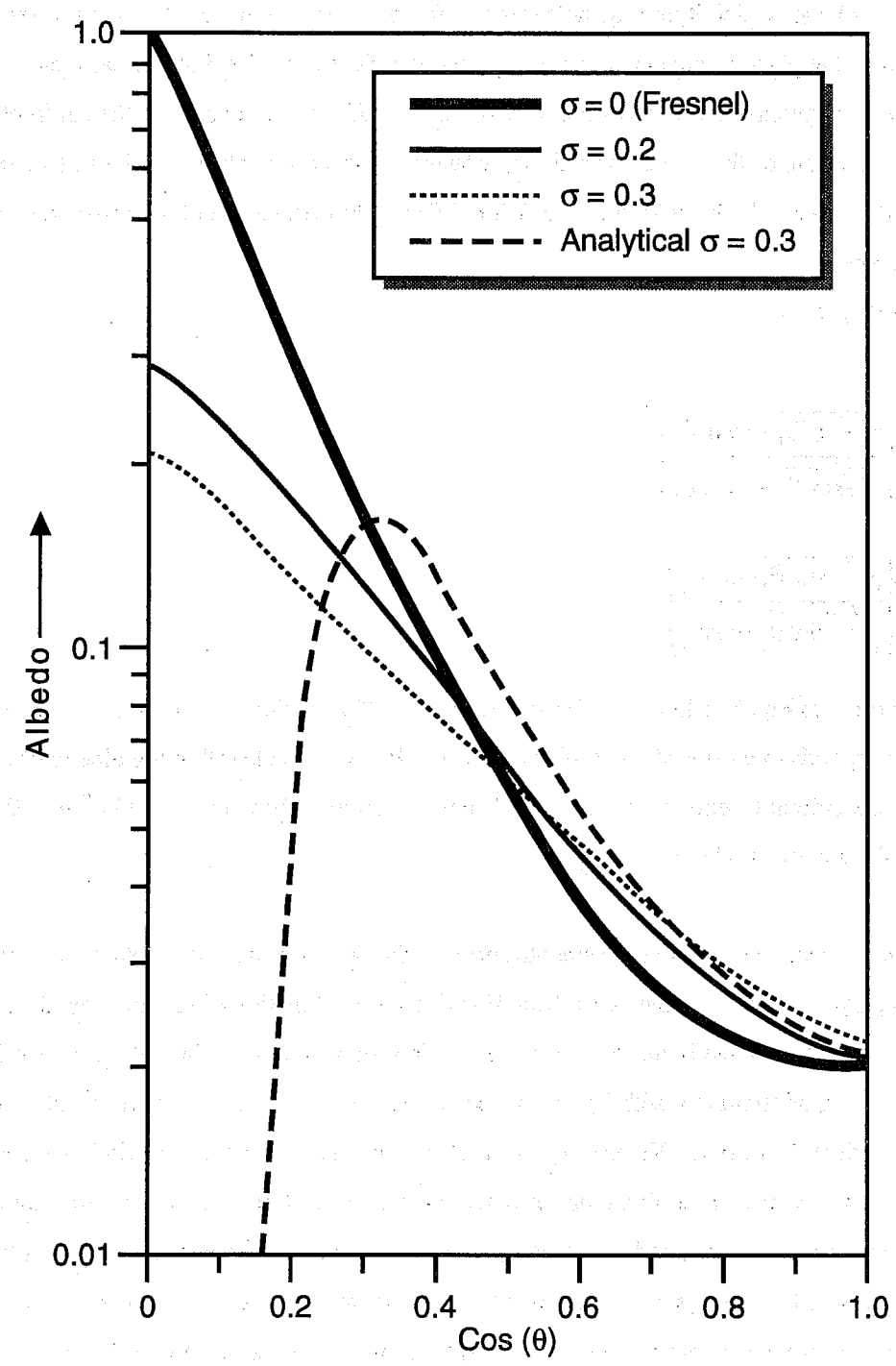

Fig 3 Zenith-angle dependence of reflection coefficient for a flat surface. The rough ocean surface cases (σ-0.2, 0.3) are shown as well.

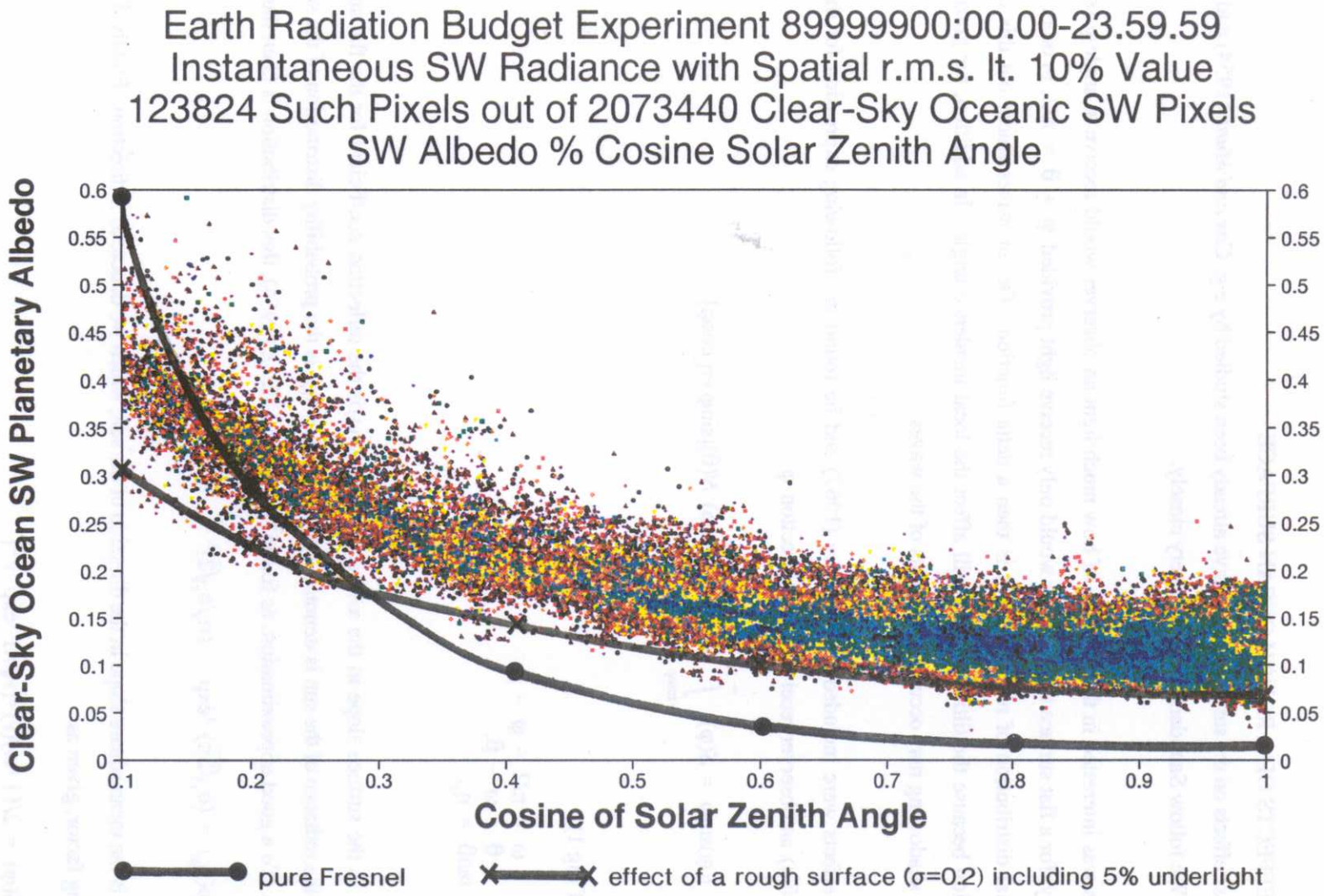

Fig 4 ERBE top of atmosphere clear sky albedo in comparison with some surface albedos.

that at higher zenith angles ($\theta > 60°$) there is a considerable scatter in the data. This could be explained by spatial variability of e.g aerosols resulting in additional reflection. In the next section we argue this scatter may also be related to the sea state dependence of the reflection.

3. EFFECTS OF A ROUGH OCEAN SURFACE

Roughness effects on the surface albedo have already been studied by e.g. *Cox and Munk* (1954) and *Saunders* (1967). We follow Saunders' treatment very closely.

Saunders was interested in the problem of how much light an observer would receive at angle φ (see Fig 1). Evidently, for a flat surface the observer would only receive light provided $\varphi + \theta = \pi/2$, in other words the directional distribution of reflected light is then a delta function. Ocean waves smear out this directional distribution because the tilting surface will affect the local incidence angle. In addition, for grazing angles ($\theta \approx \pi/2$) shadowing may occur by the crests of the waves.

Shadow effects were included by *Saunders* (1967) and he found the following expression for the average radiance $I(\varphi)$ an observer receives in the direction φ

$$I(\varphi)\sin\varphi = S(\varphi) \int_{-\tan\varphi}^{\infty} d\eta_x \, p(\eta_x) \, R(\omega) \, N(\theta)[\sin\varphi + \eta_x \cos\varphi] \tag{3}$$

where (cf Fig 1)

$$\begin{aligned} \omega &= \pi/2 - \varphi - \beta, \\ \theta &= \omega - \beta, \\ \tan\beta &= \eta_x. \end{aligned} \tag{4}$$

Here, η_x is the surface slope in the x-direction and $R(\omega)$ is the reflection coefficient for the flat surface. In addition, the radiance of the sun is denoted by $N(\theta)$ while $p(\eta_x)$ is the probability distribution of the sea surface slope η_x. To a good approximation, as found by *Cox and* Munk (1954), this distribution is Gaussian

$$p(\eta_x) = (\sigma_x\sqrt{2\pi})^{-1}\exp - (\eta_x/\sigma_x\sqrt{2})^2 \tag{5}$$

where σ_x^2 is the mean square slope in the direction of the sun, which we denote as x-direction. Finally, S is a slope shadowing factor, given as

$$S(\varphi) = 2/\{1 + erf(v) + (v\sqrt{\pi})^{-1}\exp -v^2\} \tag{6}$$

with

$$\nu = (\sigma_x \sqrt{2})^{-1} \tan\varphi,$$

and $erf(x)$ is the error function.

Effects of shadowing appear in the shadow factor S, and also through the lower boundary of the integral over the slopes η_x in (3), which is $-\tan\varphi$ instead of $-\infty$.

For the case of a clear sky the expression for the radiance received by an observer simplifies considerably since this is a case of a plane wave. Because of the two-dimensional geometry the appropriate measure is the solid angle $d\Omega = d\,\theta$. Hence, a plane wave corresponds to a radiance

$$N = N_o \delta(\theta - \theta_o) \tag{7}$$

since then $\int d\Omega N = N_o$. Since incidence angle θ and surface slope η_x are related for fixed look angle φ, we may write

$$N = \frac{N_o}{|\frac{\partial\theta}{\partial\eta_x}|}\ \delta(\eta_x - \eta'_x)\ . \tag{8}$$

Because of the delta function the integration over surface slopes may be performed with the result

$$I(\varphi)\sin\varphi = \begin{cases} 0, & \tan\beta' \le -\tan\varphi \\ \tfrac{1}{2} S(\varphi)\ p(x')\ R(\omega')(1+x'^2)[\sin\varphi + x'\cos\varphi]\ N_o, & \tan\beta' > -\tan\varphi \end{cases}, \tag{9}$$

Here, the primed variables follow from the condition $\theta = \theta_o$, i.e.

$$\begin{aligned} \beta' &= \pi/4 - \tfrac{1}{2}\varphi - \tfrac{1}{2}\theta_o \rightarrow x' = \eta'_x = \tan\beta' \\ \omega' &= \tfrac{1}{2}[\pi/2 - \varphi + \theta_o] \end{aligned} \tag{10}$$

We now consider a fixed zenith angle θ_o and we study the directional distribution of the radiance $I(\varphi)$. It is convenient to introduce the angle φ_o which is the angle for which one would expect maximum intensity in the flat surface case, thus

$$\varphi_o = \pi/2 - \theta_o \tag{11}$$

We then find with $\delta\varphi = \varphi - \varphi_o$,

$$\begin{aligned} \beta' &= -\tfrac{1}{2}\delta\varphi \\ \omega' &= \theta_o - \tfrac{1}{2}\delta\varphi \end{aligned} \tag{12}$$

while

$$s \equiv x' = -\tan \tfrac{1}{2}\,\delta\varphi .$$

The radiation flux $\Phi = I(\varphi)\sin\varphi$ thus becomes

$$\Phi = \tfrac{1}{2}S(\varphi_o - 2\beta)\; R(\theta_o+\beta)\; p(s)(1+s^2)[\sin\varphi_o - s\cos\varphi_o]N_o$$

In order to see the broadening of the directional distribution of the reflected light, we make the reasonable assumption that the rms slope of the sea surface, which is typically about 0.2, is small. Outside the shadow zone ($\tan\beta' > -\tan\varphi$) we may apply a Taylor expansion assuming that β is small, except for the probability function p which is assumed to be rapidly varying. To second order in β we find

$$\Phi(\varphi_o) = \tfrac{1}{2}N_o\cos\theta_0\; S(\varphi_o)\; R(\theta_o)p(s)(1+s^2)[1+A\beta+\tfrac{1}{2}B\beta^2] \qquad (13)$$

where

$$A = -2\frac{S'}{S_o} + \frac{R'}{R_o} - \tan\theta_o$$

and

$$B = 4\frac{S''}{S_o} - 4\frac{S'R'}{S_oR_o} + \frac{R''}{R_o} + 2\tan\theta_o\left(2\frac{S'}{S_o} - \frac{R'}{R_o}\right)$$

Here, $S'_o = \partial S/\partial\varphi_o$, $R'_o = \partial R/\partial\theta_o$, etc. We note from (13) the broadening of the directional distribution due to finite steepness. In the limit of vanishing steepness, $\sigma_x \to 0$, we recover the case of reflection from a flat surface. Finite steepness gives a broadening according to a Gaussian; the linear term in β gives an asymmetry, so that the maximum flux is not in the direction φ_o.

4. ALBEDO CALCULATION

Saunders' principal interest was in the amount of light received at angle φ. We, on the other hand, are interested in the reflected vertical energy flux from a rough surface, which requires integration of the flux $\Phi(\varphi)$ over the solid angle $d\varphi(0 \le \varphi \le \pi)$. When normalised by the incoming solar flux (which is in fact $N_o\cos\theta_o$), this gives the ocean surface albedo needed for the radiation scheme of an atmospheric model.

One can derive an analytical expression for the albedo based on Eq (13) which is valid for small steepness, outside the shadow zone. Using (13) the albedo A is then found to be (neglecting shadowing)

$$A = R_o(1+\tfrac{1}{2}B\sigma_x^2) \tag{14}$$

Substituting B we find explicitly

$$A = R_o\left(1+\tfrac{1}{2}\sigma_x^2\left\{\frac{R''}{R_o}-2\tan\theta_o\frac{R'}{R_o}\right\}\right) \tag{15}$$

From Fig 3 we infer that both R' and R'' are positive. Hence, for small zenith angle θ_o (when $\tan\theta_o$ is small) one should expect an enhancement of albedo in the presence of ocean waves while for grazing angles a reduction of albedo is expected. We remark, furthermore, that there is an evident need for the introduction of shadowing for grazing angles since $\tan\theta_o \to \infty$ for $\theta_o \to \pi/2$. It therefore seems more realistic to consider the full expression for the vertical flux (viz Eq (9)) and so determine the albedo numerically. Results are plotted in Fig 3 for an rms slope of 0.2 and 0.3 and Fig 3 confirms our expected enhancement for low zenith angles. For grazing angles, on the other hand, a considerable reduction of the ocean surface albedo is found when comparing results with that of a smooth surface.

We summarise by remarking that we have shown analytically and numerically that for small zenith angles, compared to the case of a smooth surface, an enhancement of albedo due to ocean waves is found, while for grazing zenith angles we have shown numerically that the albedo is reduced. Furthermore, it is emphasised that the analytical formulation (15) is only qualitatively correct. Deviations between the approximate expression (15) and the numerical result may become quite considerable, in particular for large zenith angles, as may be inferred from Fig 3.

5. UNDERLIGHT AND WHITECAPS

We have shown, based on the results obtained by Saunders, that the clear sky albedo of the ocean surface depends on the sea state.

Nevertheless, it should be pointed out that, comparing results from Fig 3 to the observations of Fig 4, there is a considerable underestimation of the albedo for low zenith angles (note that in that region there is hardly any difference between the surface albedo and the planetary albedo). This discrepancy may perhaps be resolved by taking into account the 'underlight'. It is therefore suggested to add a term

$$a(1-A),\ a \simeq 0.05 \tag{16}$$

to the albedo as determined in section 4. For σ=0.2 the resulting albedo is plotted in Fig 4 and a reasonable agreement is found. In particular, for low zenith angles we find a fair agreement between the lower envelope of the data and modelled albedo, while there is also a fair agreement on the dependence on zenith angle. Thus, a considerable improvement with respect to Fresnel reflection is obtained.

Furthermore, the effect of mean whitecaps may be included by using the empirical relation between whitecap coverage f and wind speed U_{10} of *Monahan and O'Muircheortaigh* (1986). It reads

$$f = 1.9510^{-5}\ U_{10}^{2.55}\ \exp[0.0861(T_w - T_a)]$$

where T_w and T_a are water and air temperatures.

Note that the whitecap coverage is a very sensitive function of wind speed (for $U_{10} = 5$ *m/s*, $f \approx 1‰$ while for $U_{10} = 25$ *m/s*, $f \approx 7$ %. Estimating the albedo of foam, r_{foam}, by a constant, $r_{foam} \approx 0.3$, the total albedo then becomes

$$A_{tot} = f\ r_{foam} + (1-f)A \qquad (17)$$

To investigate the impact of whitecaps on the ocean surface albedo we performed a test with 1 day of ECMWF wind fields U_{10} and we used the empirical relation found by *Cox and Munk* (1954) between mean square slope and wind speed.

$$\sigma_x^2 = ½(0.003 + 0.00512\ U_{10}) \qquad (18)$$

where the expression between the brackets is the total mean square slope as found in the field. Assuming an isotropic ocean surface we take half of the total mean square slope. Hence we took 1 day of wind fields and we generated using (18) the ocean surface albedo A and A_{tot}. Results are given in Fig 5. Comparing the two we find hardly any difference except for low zenith angles where whitecaps may apparently give an additional scatter in the albedo. We decided to retain the effect of whitecaps because it has impact on the cloudy albedo, as will be seen in a moment.

Finally, it is of interest to discuss possible sea state dependence of the surface albedo in cloudy conditions. The cloudy case is defined here as the one having a uniform incoming radiance in three dimensions which means that in two dimensions $N(\theta) = N_o \sin(\theta)$. The cloudy albedo may be obtained by integrating the clear sky results over θ with solid angle $d\ \theta$. In the absence of underlight and whitecaps the wind speed dependence of the cloudy albedo (again using (18)) is given in Fig 6a.

Fig 6a shows a slight decrease of albedo with increasing wind speed in agreement with Monte Carlo simulations (cf *Mobley* (1994), p 192). Including the whitecaps (see Fig 6b) reverses the trend, however. We therefore decided that it has some relevance to include the effects of whitecaps in the calculation of the albedo.

6. IMPACT ON THE ATMOSPHERIC STATE

Based on the results of the previous sections we developed a fast and efficient algorithm to determine the ocean surface albedo. Since at present no mean square slopes from the WAM model are available during the atmospheric

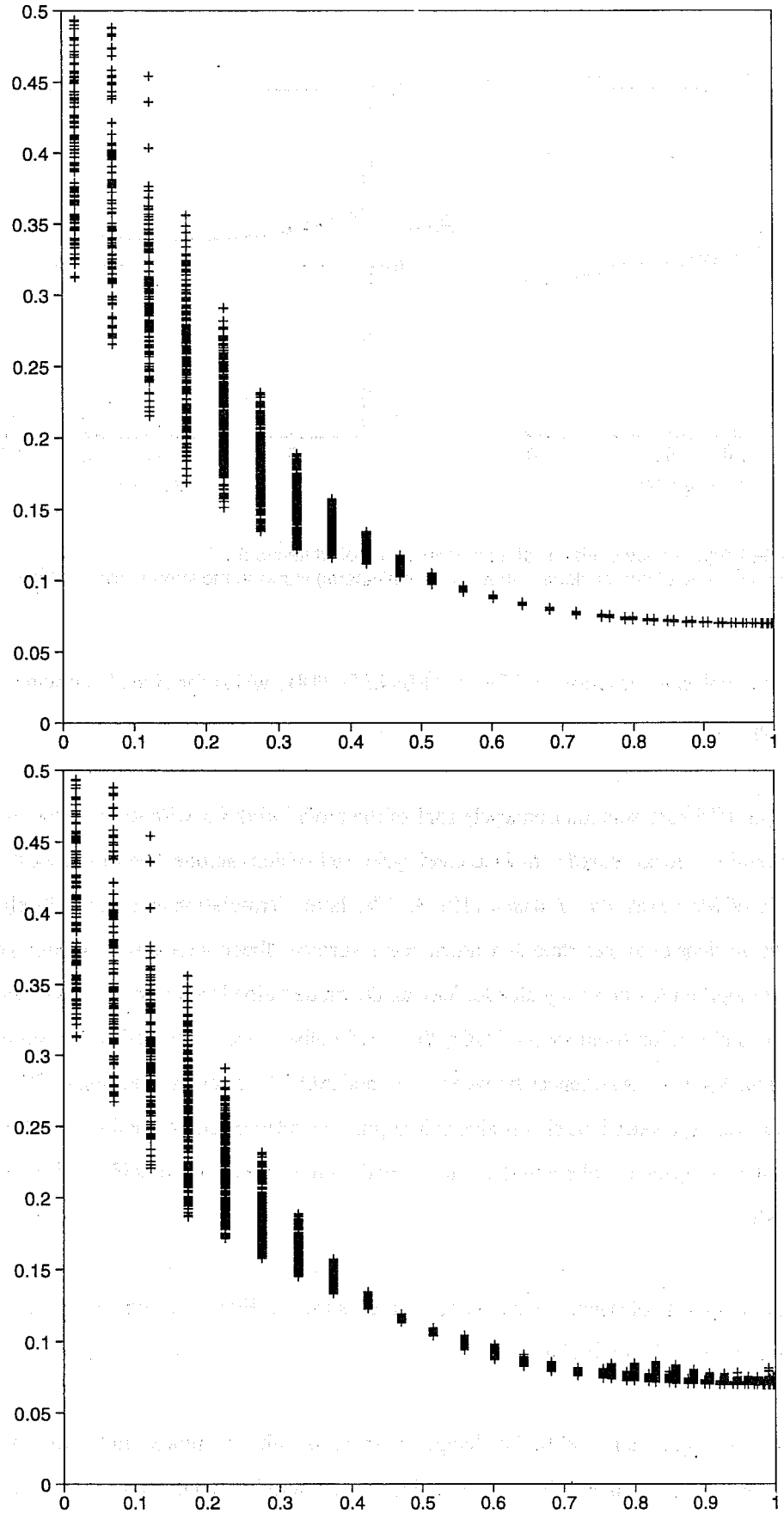

Fig 5 Albedo generated by ECMWF winds. Top: without whitecaps; bottom: with whitecaps.

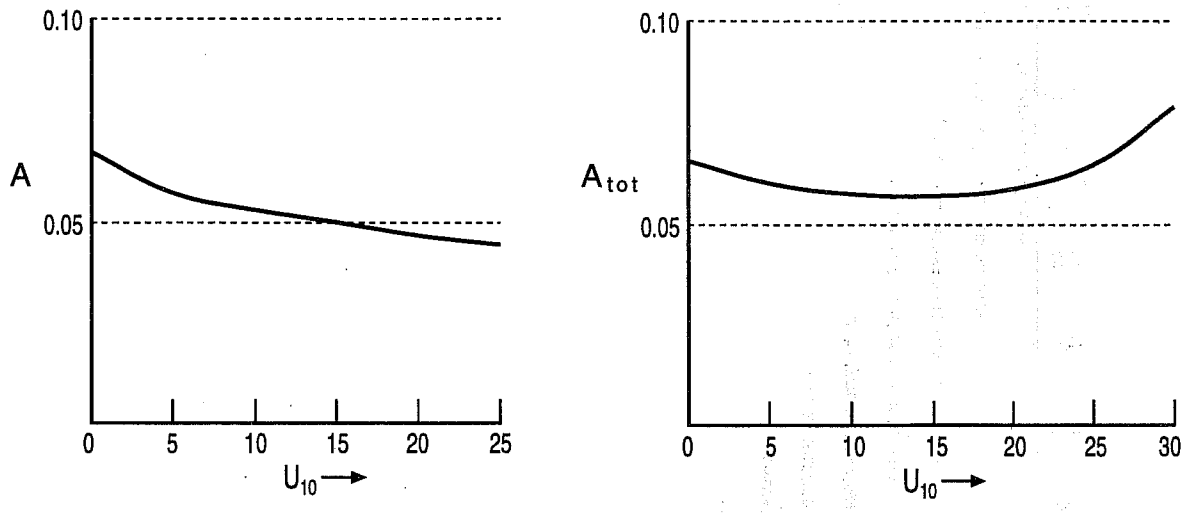

Fig 6 a: Wind speed dependence of cloudy albedo (in absence of whitecaps)
b: Wind speed dependence of cloudy albedo (with whitecaps) showing the importance of whitecaps!

forecast, we used the simple parametrization of Cox and Munk (Eq (18)), which for given local wind speed U_{10} gives the mean square slope.

A one year simulation at T63L31 was run from cycle 13r1 of the model libraries with the sea-state dependent ocean surface albedo and results were compared with the control cycle 13r1 which includes the formulation of the sea-state independent albedo of *Morcrette and Janssen* (1995). The latter formulation of albedo closely resembles the Fresnel albedo. Two versions of the sea state dependent ocean surface albedo were tested. In one version (denoted as AOC//) we only modified the clear sky albedo, leaving the cloudy albedo unchanged to its value in cycle 13rl ($\simeq 0.07$). In the second version (denoted as AOC), the cloudy albedo was also modified in agreement with the results of the previous section. Differences between AOC and AOC// are regarded as small. The reason for this is that when white caps are introduced the cloudy albedo is in practice independent of wind speed. We therefore only discuss results of the experiments where both clear sky and cloudy albedo are modified, although results of all 3 experiments are shown.

Results are presented in terms of zonal means over the ocean surface. Figs 7a-c compare the annually averaged components of the surface radiation budget.

The response of the atmospheric model to the change in albedo is rather complex. In the Southern Hemisphere extra-tropics there is hardly any change in long wave radiation and there is a small increase in short wave radiation (note that the sign convention is such that a negative flux means transport from ocean to atmosphere). On the other

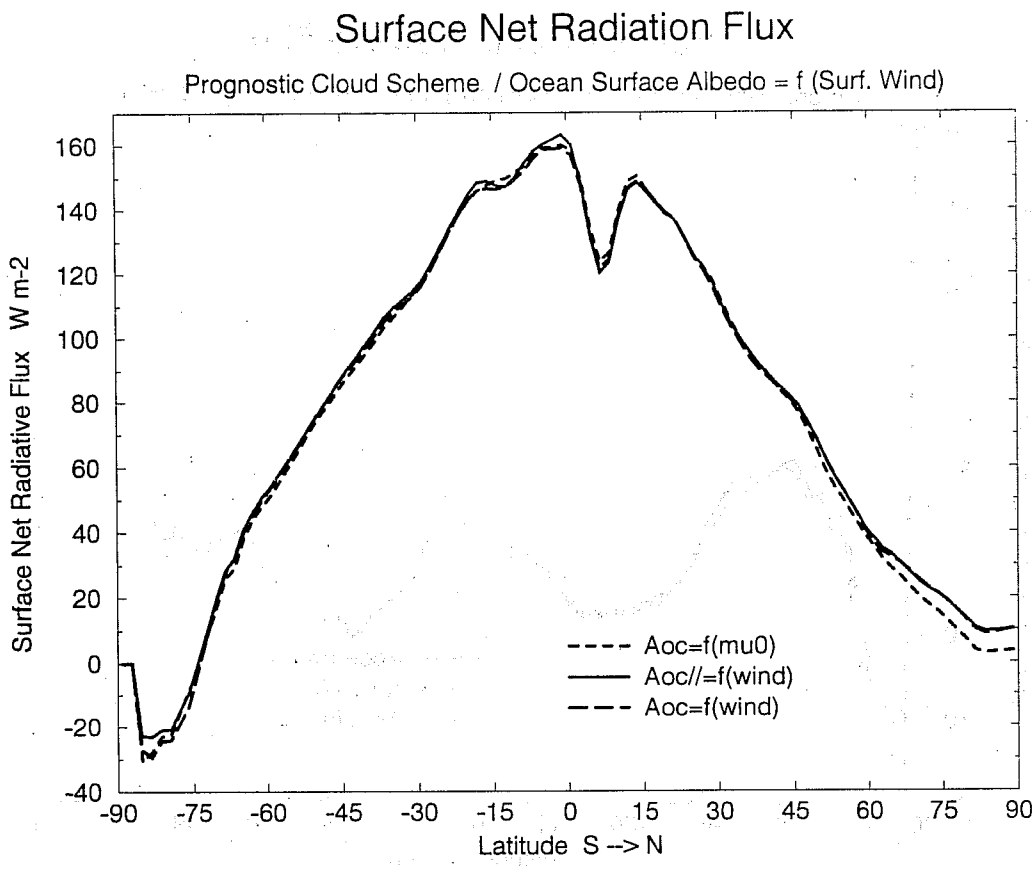

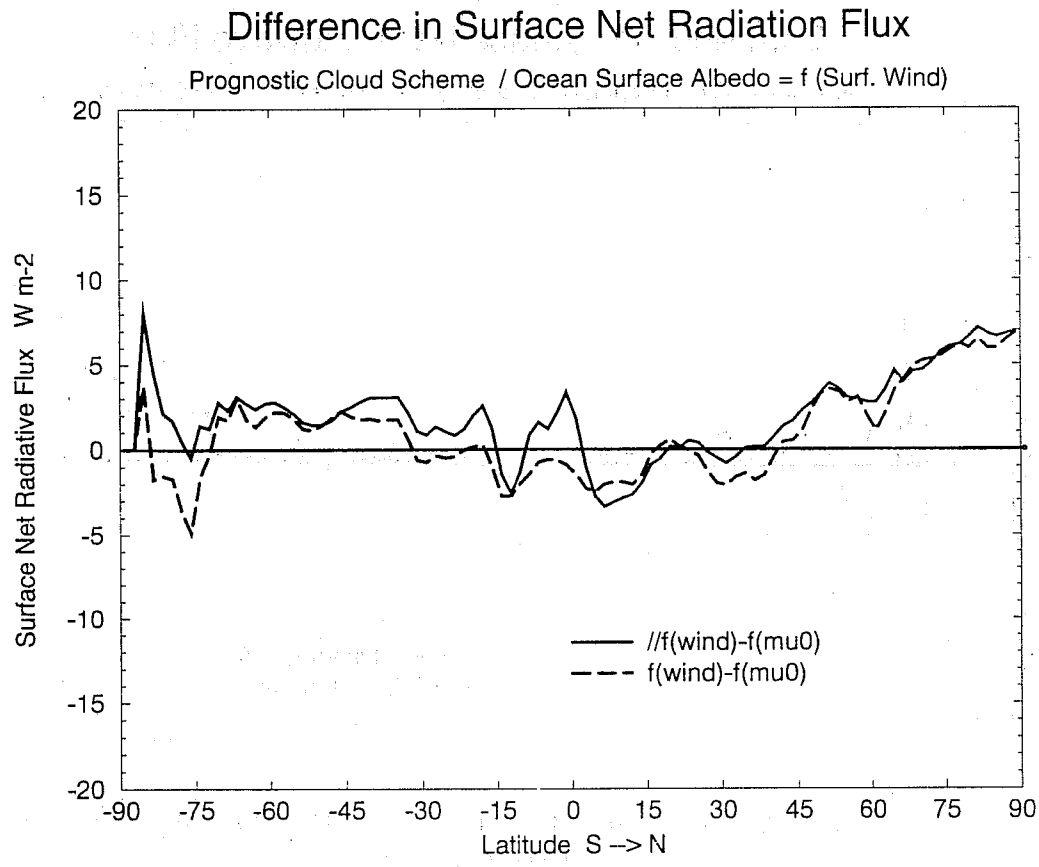

Fig 7a Zonal, one year average at ocean surface of net radiation flux and their differences.

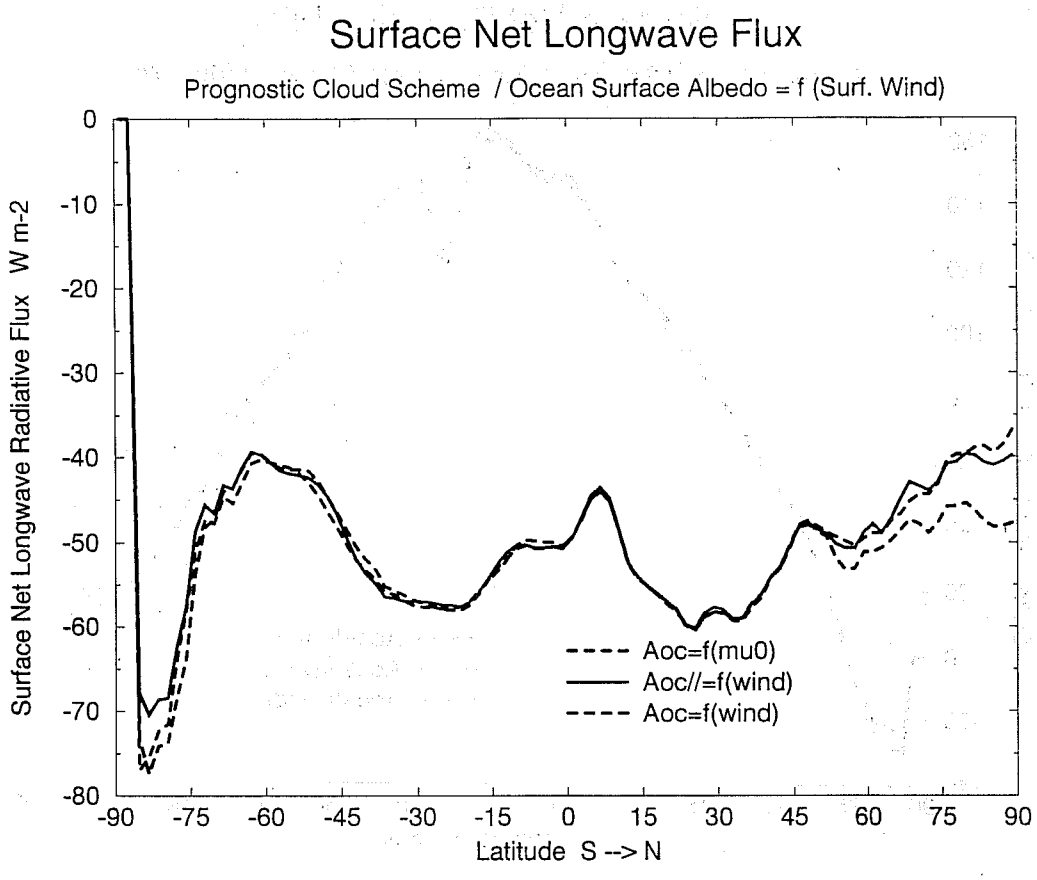

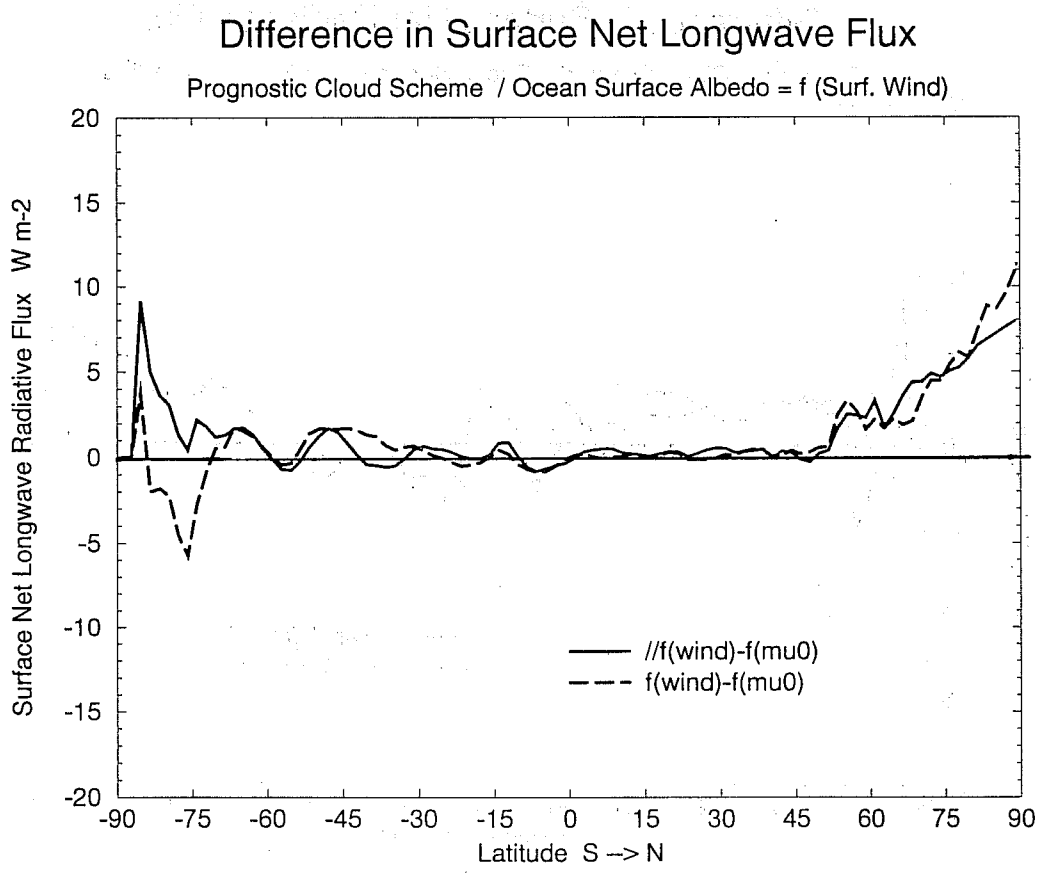

Fig 7b Zonal, one year average at ocean surface of net long wave flux and their differences.

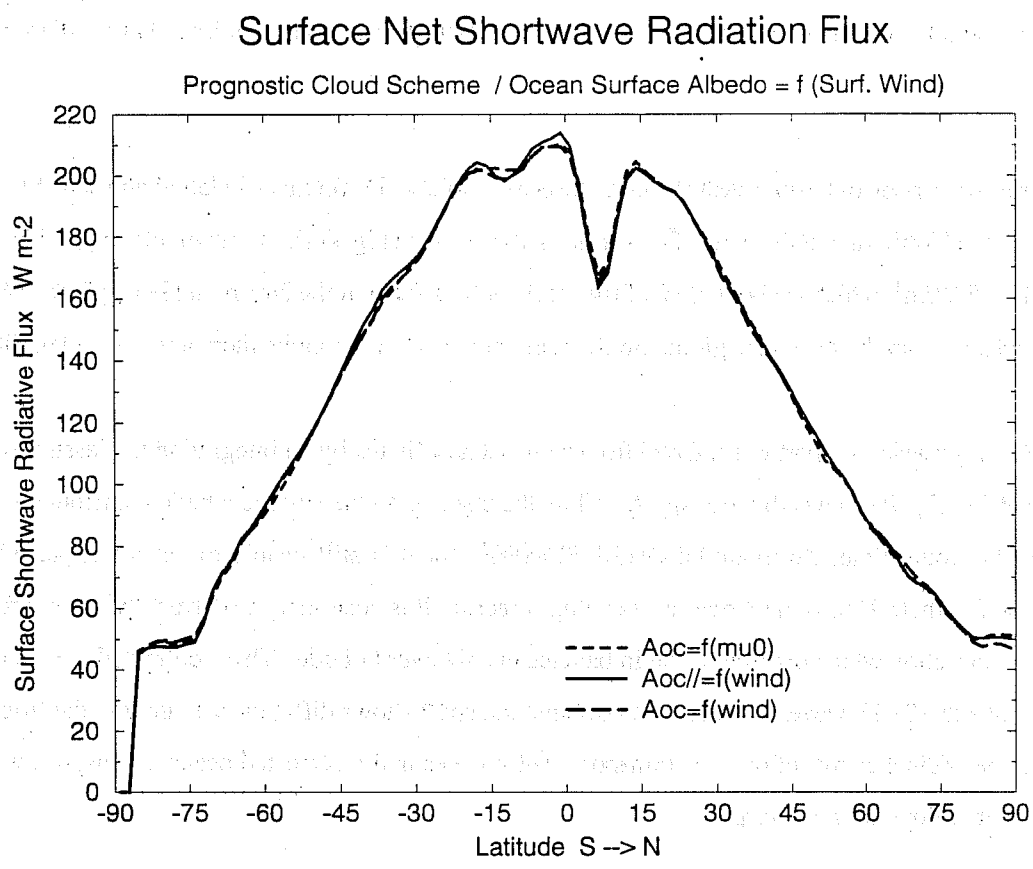

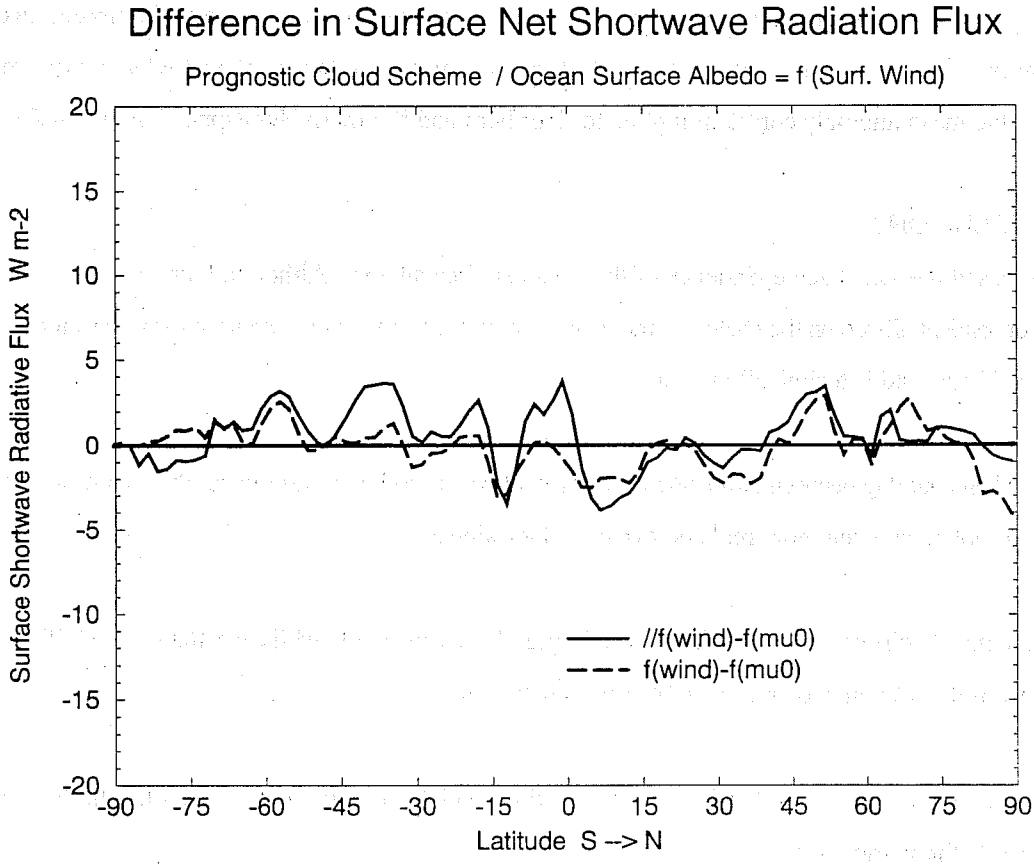

Fig 7c Zonal, one year average at ocean surface of short wave flux and their differences.

hand, in the Northern Hemisphere extra-tropics (north of 45° N) there is reduction in long wave radiation of about 5 W/m^2.

Fig 8 presents a comparison of the turbulent fluxes at the ocean surface. Differences in latent and sensible heat flux occur mainly in the Northern Hemisphere. The surface net heat flux (Fig 9) shows relatively large differences (of the order of 10-15 W/m^2, which is about 50% of the total net heat flux) in the Northern Hemisphere but these are confined to a relatively small area of the globe. In the remaining part of the globe there are only small differences.

The corresponding oceanic transport was inferred from these net heat fluxes by an integration that assumes zero flux at the North Pole. Fig 10 shows this transport. While the changes to the surface albedo contribute to a smaller imbalance at the South Pole, the modified cy13rl ECMWF model is still unable to get the expected negative transport in the Southern Hemisphere over a year-long forecast. It is customary to correct the curves for oceanic transport by a correction which distributes the imbalance evenly over latitude. These corrected curves are shown at the bottom of Fig 10. However, the corrected oceanic transport shows differences mainly in the tropics which are not seen in the original curves of oceanic transport. Differences in the corrected oceanic transport, while being quite large, are therefore hard to interpret.

Furthermore, a number of 10 day forecasts were performed using starting dates equally distributed over the four seasons. However, because of the modest impact seen in the climate simulation, no impact was expected. This is confirmed by the mean anomaly correlation plots for Northern and Southern Hemisphere shown in Fig 11.

7. CONCLUSIONS

We have discussed the sea-state dependence of the ocean surface albedo. Although there is hardly any impact of the sea-state dependent albedo on the mean weather state, we prefer to introduce the new formulation because it has a clear physical basis and is technically feasible.

Furthermore, when coupling between atmospheric model and wave model is introduced, the root mean square slope may be used to obtain an even more realistic ocean surface albedo.

Acknowledgment: A discussion with Nils Wedi is greatly appreciated, while we thank A Hollingsworth for suggestions for improvements to an earlier draft of this memo.

Remark: This memo replaces results of earlier calculations which were wrong because they did not concern the albedo referred to the vertical flux.

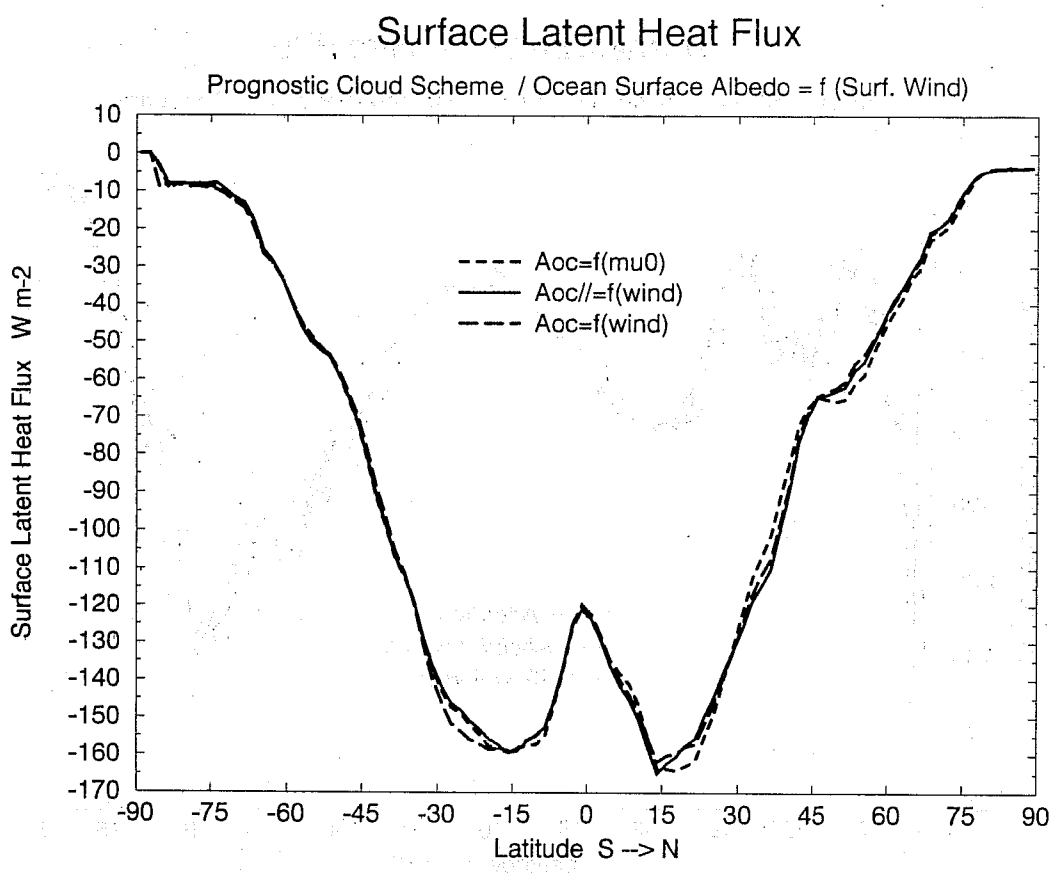

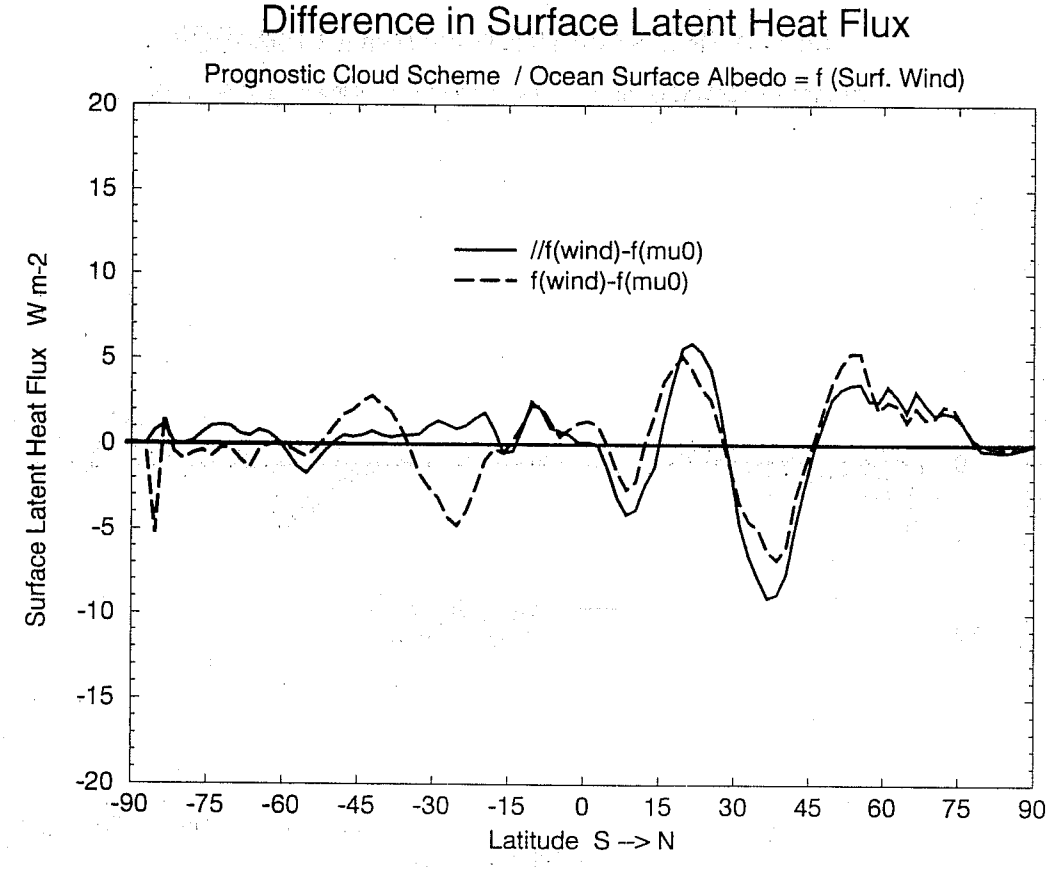

Fig 8a Zonal, one year average at ocean surface of latent heat flux and their differences.

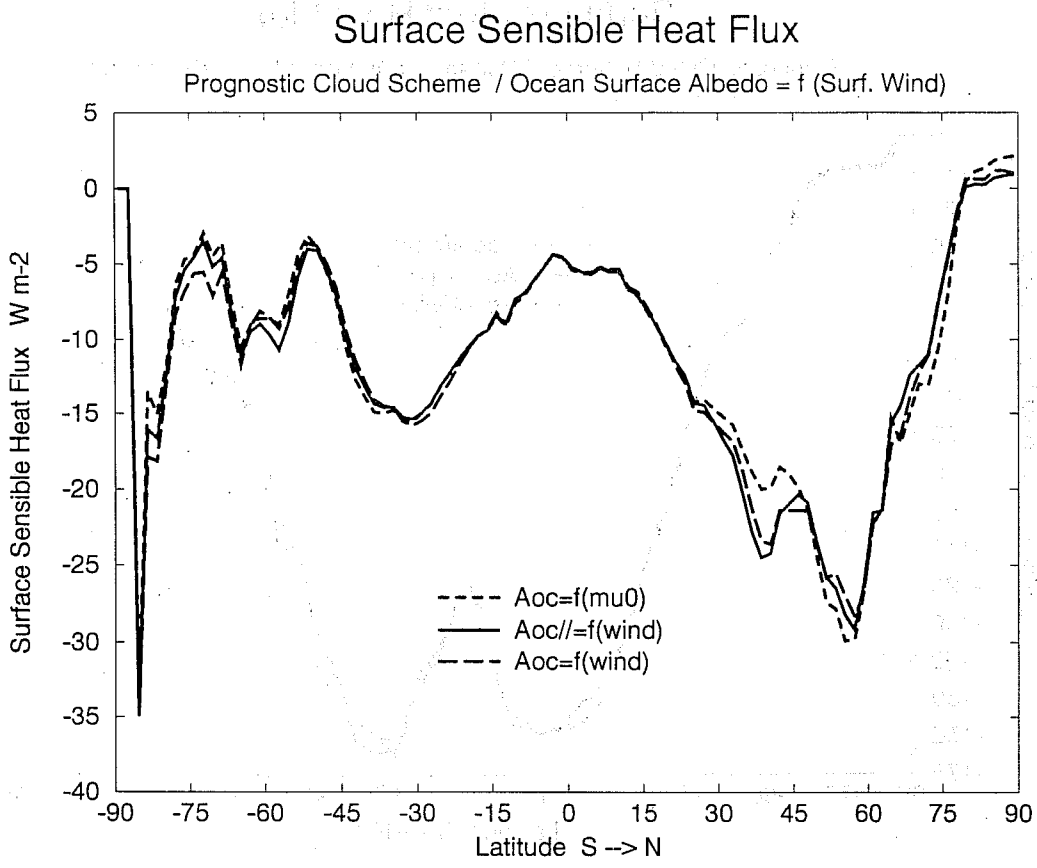

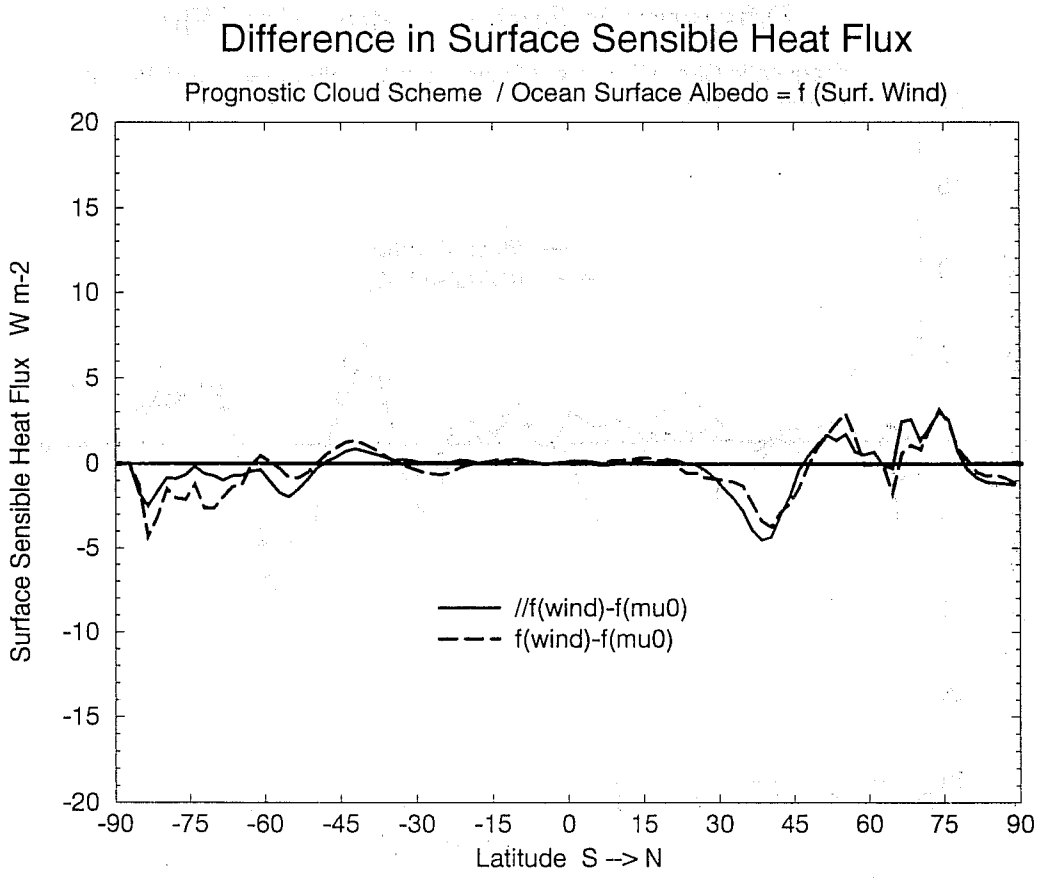

Fig 8b Zonal, one year average at ocean surface of idem for sensible heat flux.

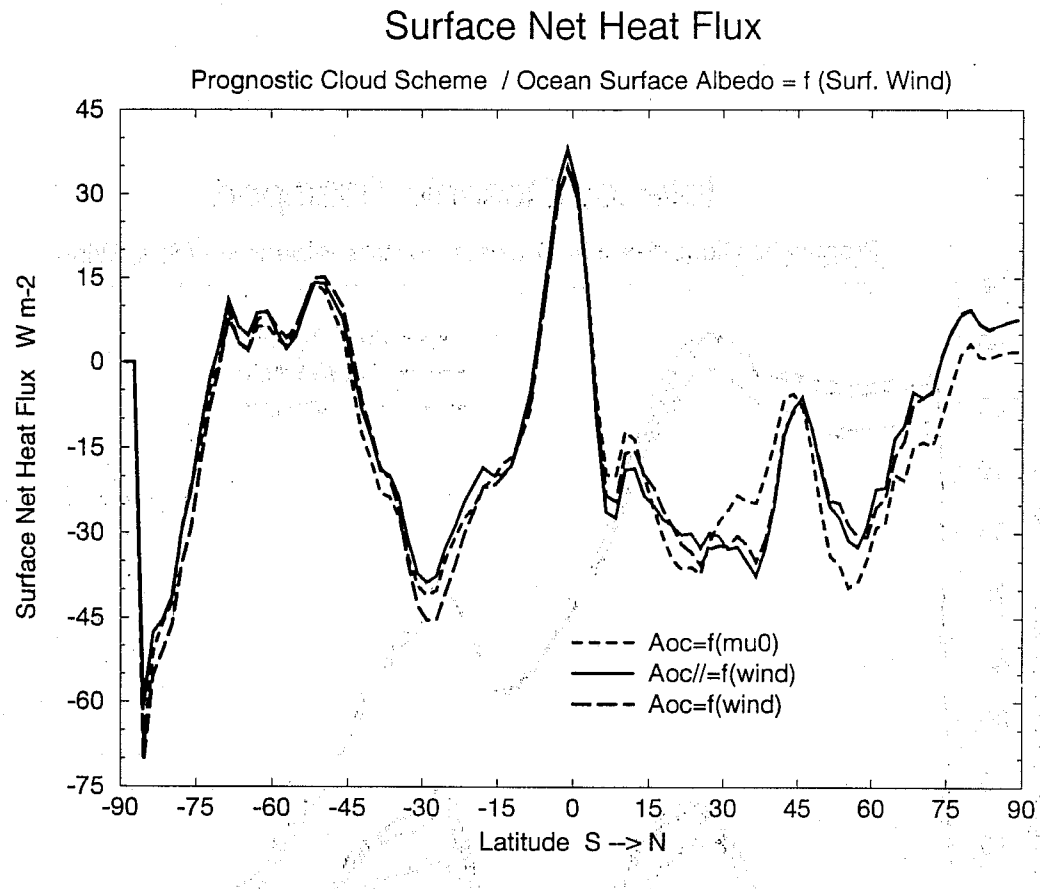

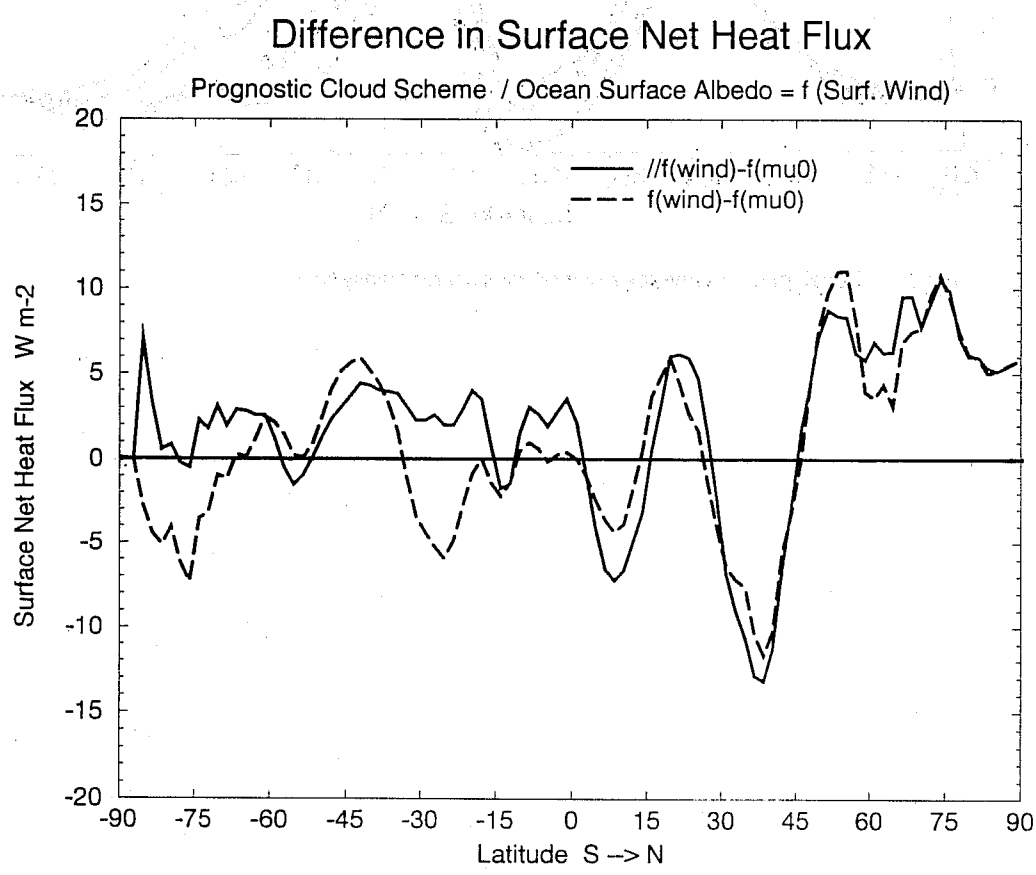

Fig 9 **Zonal, one year average at ocean surface of net heat flux and their differences.**

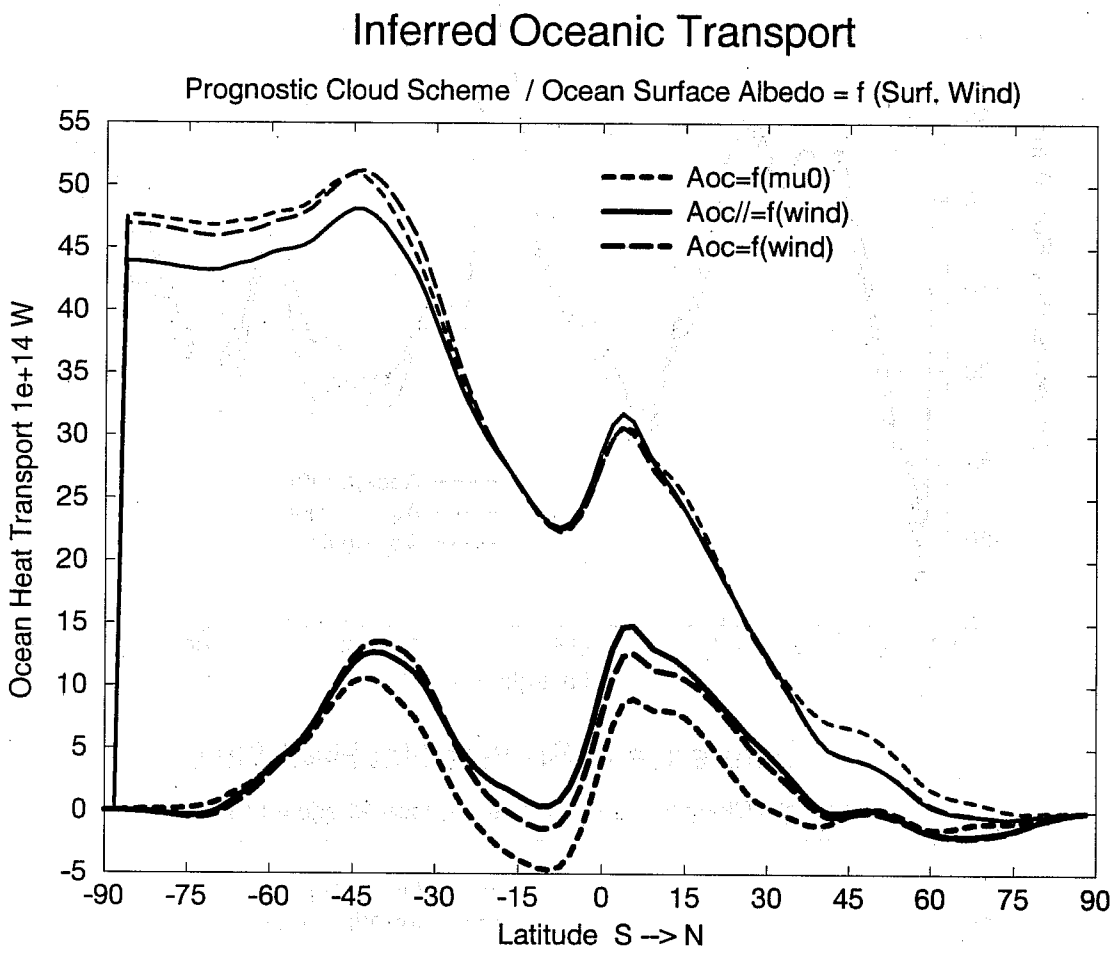

Fig 10 Zonal, one year average of inferred oceanic transport.

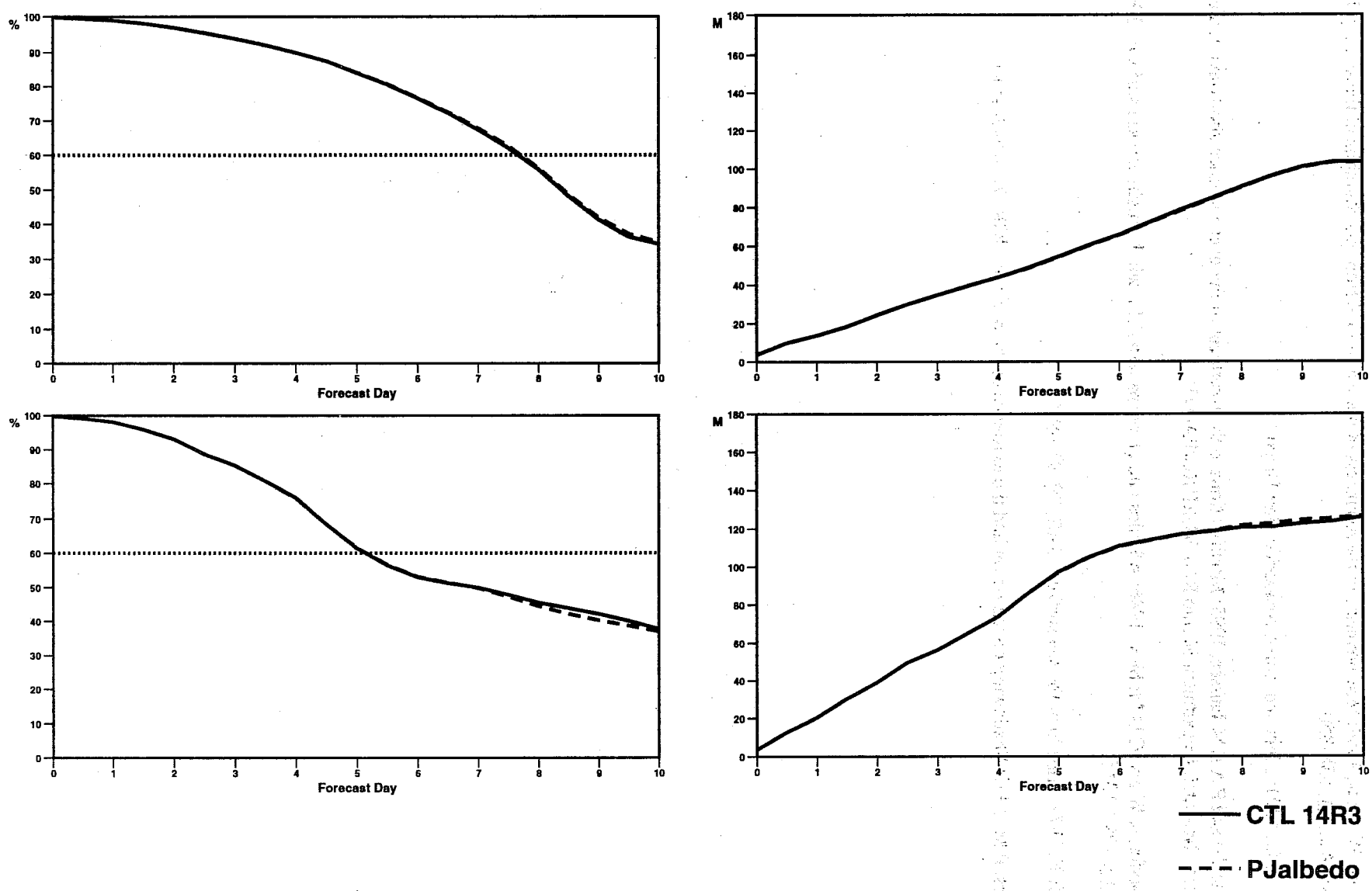

Fig 11 Anomaly correlation and rms forecast error averaged over 4 cases showing that on the 10 day forecast the difference between sea-state dependent albedo and control (14R3) is minimal.

REFERENCES

Cox, C and W Munk, 1954: Measurements of the roughness of the sea surface from photographs of the sun's glitter. J Opt Soc Am, 44, 838-850.

Mobley, C D, 1994: Light and water, Academic, San Diego.

Morcrette, J-J and P A E M Janssen, 1995: Modifications to the treatment of the ocean surface shortwave radiative properties. Research Department Memo R60.9/JJM/103/PA/WV.

Preisendorfer, R W and C D Mobley, 1986: Albedos and glitter patterns of a wind-roughened sea surface. J Phys Ocean, 16, 1293-1316.

Payne, R E, 1972: Albedo of the sea surface. JAS, 29, 959-970.

Saunders, P M, 1967: Shadowing on the ocean and the existence of the horizon. JGR, 72, 4643-4649.